REU PROGRAM IN INTERDISCIPLINARY MATERIALS RESEARCH

Research Reports by Students Supported by the REU Site: Interdisciplinary Materials Research for Undergraduates (NSF REU Site Program, DMR-1757420)

This REU Program for Interdisciplinary Materials Research is co-organized and co-supported by the REU Site for Interdisciplinary Materials Science (NSF REU Site Program, DMR-1757420) and the Cornell Center for Materials Research (NSF MRSEC program, DMR-1719875). This document contains the reports by all students that were funded by the REU Site.

TABLE OF CONTENTS

STUDENT	FACULTY ADVISOR	PAGE
• Marcus Choates	Prof. Amal El-Ghazaly	3
• Santiago Vargas-Daniels	Profs. Kin Fai Mak & Jie Shan	8

Designing a Magnetorheological Elastomer for Microwave Absorption

Marcus Choates

Introduction

As remarkable as advanced telecommunication technology of the last several decades has been, it has created some new serious issues we must address if we want to keep using these devices. As far as military and mass tele-networking are concerned, telecommunication technology has created vast amounts of electromagnetic noise pollution and has created incredible amounts of electromagnetic interference and leakage in signaling. So essentially, the more we have created these devices and established these cellular networks the harder it has become to communicate. One way to combat this is to use a material that absorbs this electromagnetic leakage and pollution and one of the most notable is a magnetorheological elastomer.

A Magnetorheological Elastomer (MREs) is an elastic polymer matrix that contains added magnetic filler particles within them. In our case, those magnetic filler particles are FeCo nanocubes. When making an MRE to induce anisotropy, which is the alignment we desire, we cure the mixture of elastomer and nanoparticles under a magnetic field, which aligns the particles. In this paper, the properties of the MREs synthesized are detailed along with resonance frequency properties.

Synthesis

We synthesize the nanoparticles via a polyol reaction. First we take $FeCl_3$ and $(CoCH_3CO_2)_2$ and mix them in Ethylene Glycol. We stir this mixture for 30 min.

Next we add NaOH to reduce the compounds in the solution from their ionic forms to their neutral elemental forms. While the entire mixture is stirring, any Ethylene Glycol that is evaporated is condensed by a constant stream of running water through a column fixed to the top of the flask. After we have added the NaOH we let in react and reflux for about 1 hour and then extract the FeCo nanocubes via a syringe. (See figure 1.).

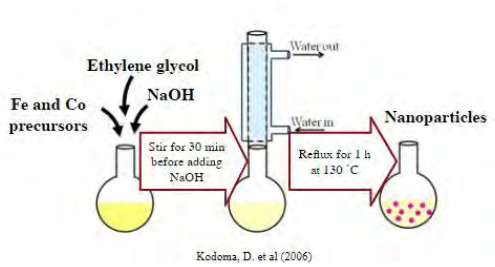

Figure 1. (Synthesis Process of FeCo nanocubes.)

The resulting nanoparticles (FeCo nanocubes) have an average size of about 62 nm. (See figure 2.).

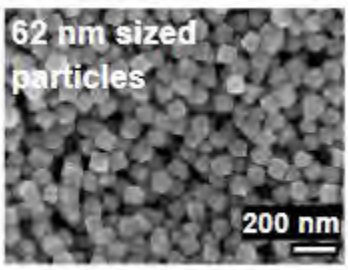

Figure 2. (SEM image of synthesized FeCo nanocubes.)

Fabrication

We fabricated our magnetorheological elastomers via mixing our synthesized nanoparticles with a silicone, Ecoflex , at a concentration of both 3 and 8 vol% (with

respect to the overall volume of the mixed components).

To detail further, when we fabricate our magnetorheological elastomer, we take the FeCo nanocubes and mix them manually into “Ecoflex Part A” and Silicone Thinner from “Smooth on” (i.e. stirred with a stirring rod) until the powder was fully disperses in the mixture. Then, in order to fully disperse the particles and break agglomerates the mixture is then ultrasonicated at 40kHz and 180W at room temperature for 2 minutes. Next add we Ecoflex Part B to the mixture after sonication and manually stir (with a stirring rod.). Next, we apply a demolding agent (release agent) to a custom-made aluminum mold in order to help ease the remove of the finished MRE. The demolding agent was left to dry for 5 mins. Then mixture was poured into a custom-made aluminum mold with a cavity of diameter 2.5 in. After this the composite was degassed in a desiccator for 2 minutes. Then, the covered mold was vacuum-sealed in a plastic bag in order to uniformly press the cover and make 2.5 in. Lastly, the mixture was cured for 4 hours under a uniform magnetic field of 350mT. (See figure 3.).

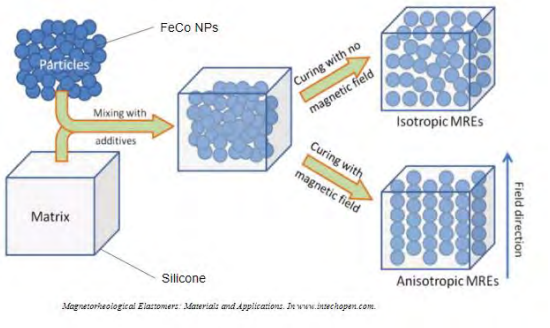

Figure 3.(Fabrication of the Anisotropic Elastomer.).

Characterization

After fabricating our sample, we then test it using a vector network analyzer (9123 Agilent 8722ES 40GHz Network-Analyzer) for characterization.

A vector network analyzer (VNA) is a device in which we used to send microwaves through our into our system for study. (See figure 4.). For fabrication we connect a printed circuit board (in this case a y-coupler with two connected waveguides) to the VNA. This printed circuit board is the area of which we place our samples on to absorb the microwaves. Incoming microwaves, generated from the left port (Port 1) have passed through the printed circuit board are measured in the right port (Port 2). (See figure 5.). We measure two parameters from the VNA: S_{11} data and S_{21} data. S_{11} measures how much power is reflected at Port 1. S_{21} measures how much power is received at Port 2. The mathematical difference (S_{21} - S_{11}) is the amount absorbed into the MRE.

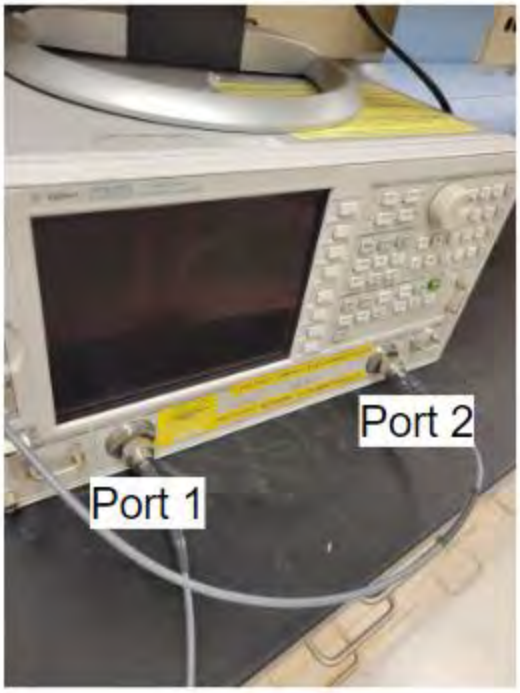

Figure 4. (The 9123 Agilent 8722ES 40GHz Network-Analyzer and its ports).

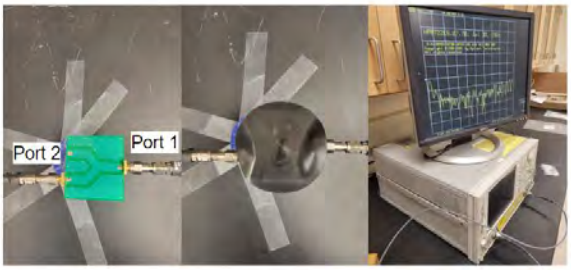

Figure 5. (The Fabrication Process).

We tested 5 different samples: one test without a sample (No Sample), one test with one layer of the 3 vol% MRE, one test with three layers of the 3 vol% MRE, one test with six layers of the 3 vol% MRE, and one test with one layer of the 8 vol% MRE. (See figures 6-10).

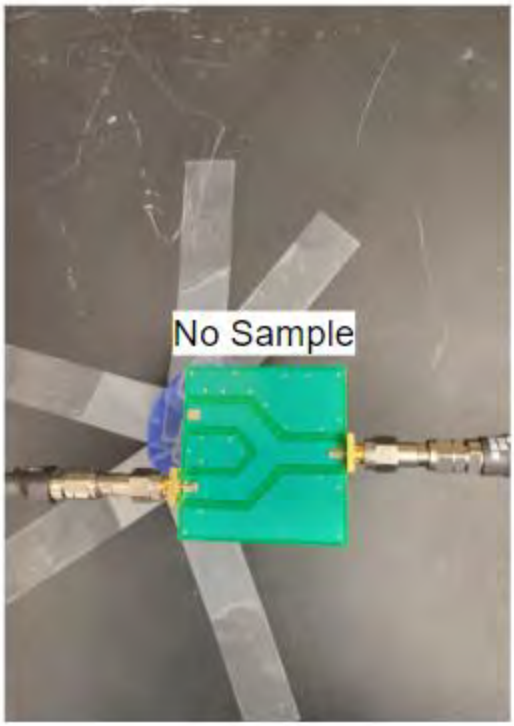

Figure 6. (No Sample)

Figure 7. (One layer of the 3 vol% MRE).

Figure 8. (One test with three layers of the 3 vol% MRE).

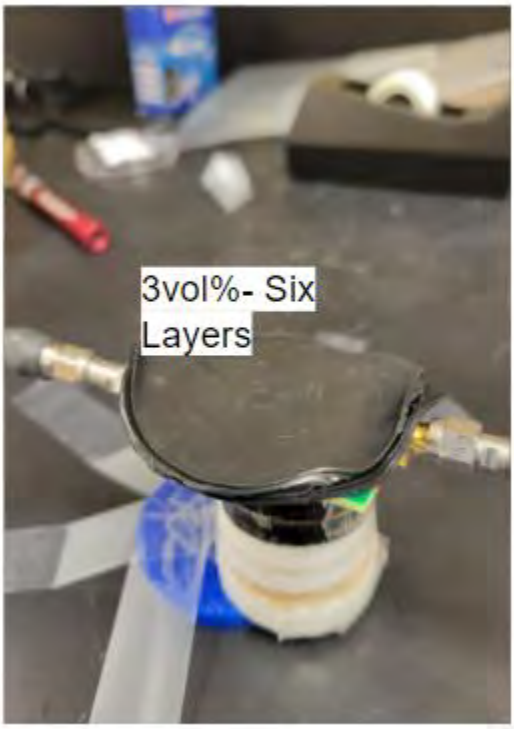

Figure 9. (one test with six layers of the 3 vol% MRE).

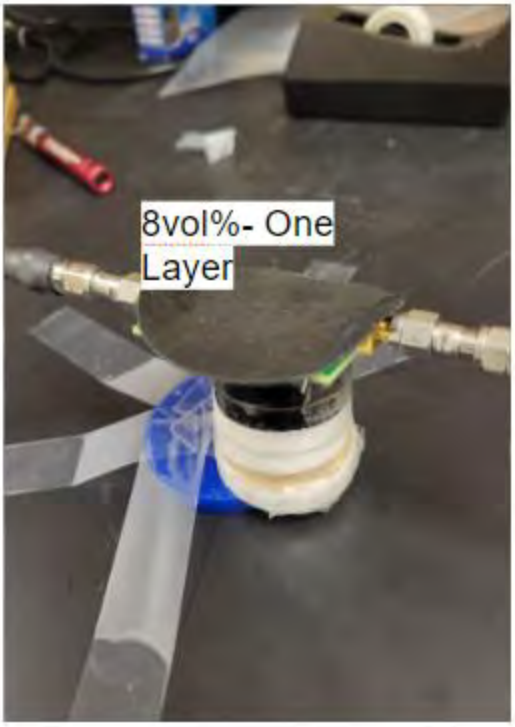

Figure 10. (One layer of the 8 vol% MRE)

Results

We did not find a discernible trend within our graphs of absorbance. We did, however, find a trend with the resonance frequency seen in the S21 measurements. The material is, more so, acting like a filter, restricting some of the incoming wave from passing through, which reduces the frequency measured at Port 2.

This gives us the same application for the material, but simply a different means of achieving it.

Conclusion

To conclude, the MREs tested didn't not act in how we hypothesized them to. However, the tested MREs' new found resonance frequency properties are still rather novel as a potential solution for the electromagnetic noise pollution. In addition to working quite

well in its intended application, these resonance frequency findings could shed new light on new areas of potential research if further experimentation is carried out.

References

Cestarollo, L., Smolenski, S., & El-Ghazaly, A. (2022). Nanoparticle-Based Magnetorheological Elastomers with Enhanced Mechanical Deflection for Haptic Displays. *ACS Applied Materials & Interfaces*, *14*(16), 19002–19011. https://doi.org/10.1021/acsami.2c05471

Cvek, M., Moucka, R., Sedlacik, M., Babayan, V., & Pavlinek, V. (2017). Enhancement of radio-absorbing properties and thermal conductivity of polysiloxane-based magnetorheological elastomers by the alignment of filler particles. *Smart Materials and Structures*, *26*(9), 095005. https://doi.org/10.1088/1361-665x/aa7ef6

Studying moiré physics in twisted double bilayer WSe2

Santiago Vargas-Daniels[1], Jiacheng Zhu[1,2], Patrick Knuppel[1,3]

[1]Department of Applied and Engineering Physics, Cornell University, Ithaca, NY, USA 14853

[2]Department of Physics State University of New York at Albany, Albany, NY, USA 12203

Abstract

Moiré van der Waals heterostructures built with two dimensional semiconductor materials provide a tunable system for studying correlated electronic states in the flat miniband structures formed by the moiré potential. Our work attempts to characterize honeycomb moiré lattice physics in twisted double bilayer WSe2 using optical sensing techniques. Strong correlation effects are observed at filling factors of $\nu = -1, -2, -1/3$ *corresponding to a mott insulator, band insulator, and a generalized Wigner crystal state.*

I. Introduction

Moiré superlattice structures form when atomic lattices with different lattice constants are stacked with at an offset, or if two identical lattices are stacked at a small twist angle relative to each other.[1] Superlattice structures have longer lattice constants which form longer wavelength periodic potentials. Subjecting these potentials to Bloch's theorem results in flat isolated miniband structures near the Fermi energy. Physics in these moiré systems can be described by the Hubbard model which is a simple toy model of electron interactions on the superlattice. Hubbard model physics is characterized by a Hamiltonian with a kinetic hopping term *t* which tends to delocalize electrons and a coulomb potential term *U* which tends to localize electrons. In the limit where *U* becomes larger than *t* electrons prefer to localize, and correlation driven effects can be observed. Moiré materials can be used to study the parameter space of the Hubbard model by continuously varying the ratio of U over t. Namely by varying the twist angle (θ) changing the superlattice constant (a_m), and adjusting device layer geometry to change the band structure. Effects such as strong correlation-driven charge transfer, Mott insulating transitions have been observed in TMD heterostructures.[1] Many of the observed states can be effectively tuned by applying gate voltages across the materials. Physical properties of these systems have been studied using optical sensing techniques as well as capacitance and transport measurements, and all methods reveal insulating states at integer and fractional filling of the Moiré superlattice. Focus of past work on moiré features in two dimensional heterostructures has primarily involved triangular lattices.[2,3,4] Honeycomb lattice structures have seen little to no exploration providing a need for characterization.

Honeycomb moiré lattice structures can form when the valence band maximum (VBM) of the moiré layer is at the gamma point of the first Brillouin zone. Numerical modeling techniques have determined that the VBM is at the gamma point from bulk to bilayer in most 2H structured TMDs.[5] WSe2 is one of the TMD materials that exhibits this band structure which has not yet seen extensive study motivating further examination. In this study, twisted double bilayer WSe2 (tdWSe2) is probed using optical sensing techniques to search for correlation driven insulating states and to determine characteristics of honeycomb moiré physics.

II. Materials and Methods

Devices are usually made of graphite gates and contacts, hBN insulating layers and monolayer TMDs as shown in Fig. 1. Graphite gates and TMD layers form capacitors which

allow charge carriers to flow in and out of the moiré layer. Graphite gates on the top and bottom of the device are used tune total charge carriers and electric field independently in the sample.

All constituent flakes were exfoliated using scotch tape to separate thin layers from the bulk crystal.[6] Such tape is then firmly attached to the flat surface of a 285nm SiO_2/Si substrate. Slow separation of the tape from the substrate leaves behind flakes from multilayer to monolayer thickness. Each constituent layer is then identified under an optical microscope.

Samples were fabricated using the technique outlined by Wang and Meric.[7] Stamps were made of Polydimethylsiloxane (PDMS)/ polypropylene carbonate (PPC) / polycarbonate (PC) on glass slides. A thin layer of PC provides an adhesive surface to lift the flakes from the substrate. Flakes were lifted from the substrate at a temperature between 40 and 110 degrees Celsius. In general, high temperature increases the adhesiveness of PC film while decreasing its structural integrity. Devices were stacked from the top down. Occasionally an additional hBN flake was lifted first to provide a clean vdW adhesive layer.

Control over the twist angle is critical when fabricating devices designed for studying moiré physics.[8] Precise angle control was achieved using the tear and stack technique where the sample flake was cut to form two flakes then stacked on itself. Alignment of the bilayers was performed by hand to an accuracy of within 0.2 degrees. TMD bilayer flakes were cut to using an atomic force microscope tip and then stacked at a twist angle.

After all the layers were stacked on the stamp it was deposited onto Si substrate with prepatterned electrodes. Release of the stamp was done at a temperature of 200 degrees Celsius to melt the PC film onto the substrate. Remaining PC film and other residue was washed away by sequential rinsing in chloroform, acetone, and isopropanol for approximately ten minutes each.

Figure 1 below shows the layout of an optical sensing device which utilized a monolayer of WSe2 in the device structure. The monolayer has a direct bandgap between the K and K' points of the first Brillouin zone.[9] Excitons are formed at these points in momentum space by incoming photons leading to strong resonance features in the reflection spectrum. The binding energy of these excitons is sensitive to the surrounding dielectric environment which is observed in the shifting of resonance peaks on a reflection spectra. Intralayer excitons which form in the monolayer have quantized energy states resembling the Rydberg states of the hydrogen atom.

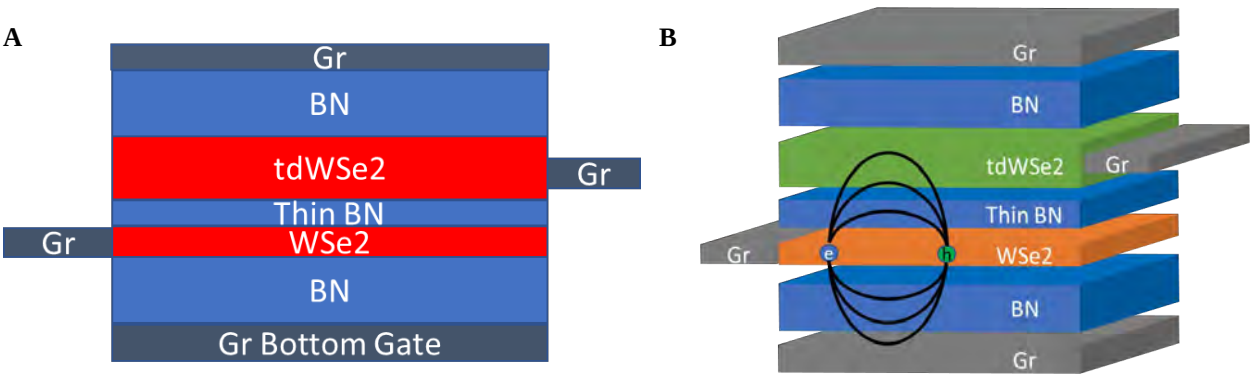

Fig. 1. (A) Two-dimensional representation of the optical sensing device geometry with graphite gates controlling the doping in the nearest TMD layer. Graphite contacts to both TMD layers are used to allow the flow of charge in and out of the sample. (B) Three-dimensional schematic of the optical sensing device showing the field lines of an intralayer exciton used for optical sensing

Higher energy states have a larger Bohr radius which results in varying sensitivity to dielectric shifts in the sample layer. In order to optimize sensitivity, the thin hBN layer in Fig. 1 is selected to be between two and five nanometers thick. In this range the 2s exciton is the most sensitive to shifts in the dielectric environment of the sample because it has a Bohr radius on the order of six nanometers.

The binding energy of the nth state exciton in the monolayer is given by

$$E_b^{(n)} = \frac{m_r e^4}{2\hbar^2(4\pi\epsilon\epsilon_0)^2\left(n-\frac{1}{2}\right)^2} \quad (1)$$

where m_r is the reduced mass of the exciton; ϵ is the dielectric constant of the uniform dielectric medium; ϵ_0 is the vacuum permittivity; e is the elementary charge; and $\hbar$ is the reduced Planck constant.[9] Resonance peaks are observed to blue shift on the spectra when the dielectric constant of the surrounding material decreases which agrees with eq. 1.

III. Results

In a 62.8 degree tdWSe2 sample the electron density at one per moiré site as calculated using a superlattice constant of 6.7 nm to be on the order of $2.47 \times 10^{12}\ cm^{-2}$. Figure 2 seen below shows a plot of the reflection contrast at a fixed back gate value of zero volts and a range of top gate values. Insulating states were observed on the hole side of the doping regime corresponding to a negative gate voltage value. Reflection contrast responses in the 2s exciton were strong at both fractional and integer filling values. When the moiré material in the device is at zero doping the system is in an insulating state corresponding to a trivial band insulator where the fermi energy sits in the bandgap. A Mott insulating state at $\nu = -1$ can be explained by the high $\frac{U}{t}$ ratio which opens a band gap at the half filling point. Long range Coulomb interactions are the dominant factor for the insulating state at $\nu = -\frac{1}{3}$ corresponding to a generalized Wigner crystal. Electron side doping shows a very weak set of features which is potentially due to contact issues with the moiré.

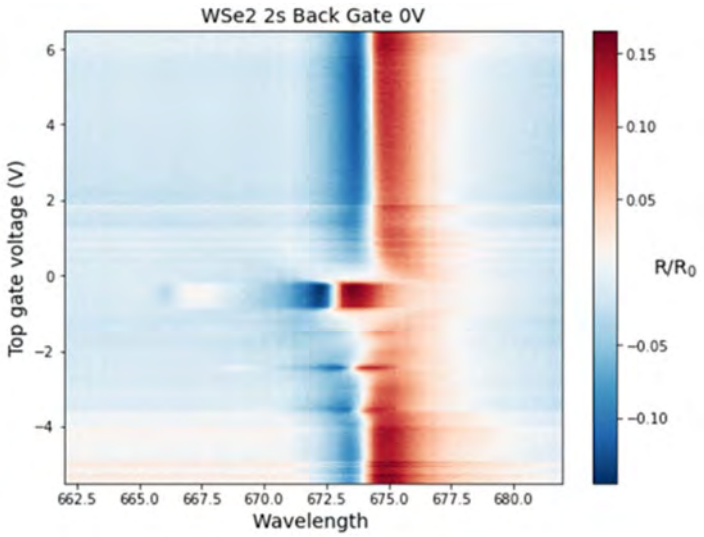

Fig 2. 62.8 degree tdWSe2 reflection spectra showing the monolayer 2s exciton for different top gate voltages, with wavelength in nm and fixed back gate (0V).

Plots at other fixed back gate voltages showed similar features prompting a need for a back gate sweep in order to confirm that the features were consistent across constant doping. Figure 3A seen below shows a dual gate sweep measurement with reflection contrast maximum

plotted to corresponding gate voltages. Lines seen on the diagonal direction represent constant doping values in the moiré material. Figure 3B shows a plot of the electric field in volts per nanometer vs the filling factor ν. Filling factors in the moiré are calculated assuming a parallel plate capacitor model using geometric capacitance between the gates and the moiré layer. Insulating states are observed to remain steady at filling factors of $\nu = -\frac{1}{3}, -1, -2$. Filling factor is observed in these graphs to have a non linear relationship to filling factor near the band edge. In this sample the band edge is located near zero electric field which can cause issues with the contact to the moiré layer due to low doping density near the contact region.

A

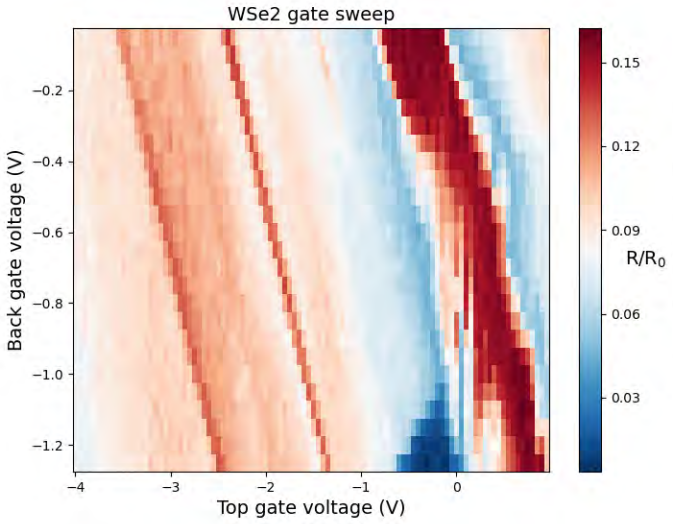

B

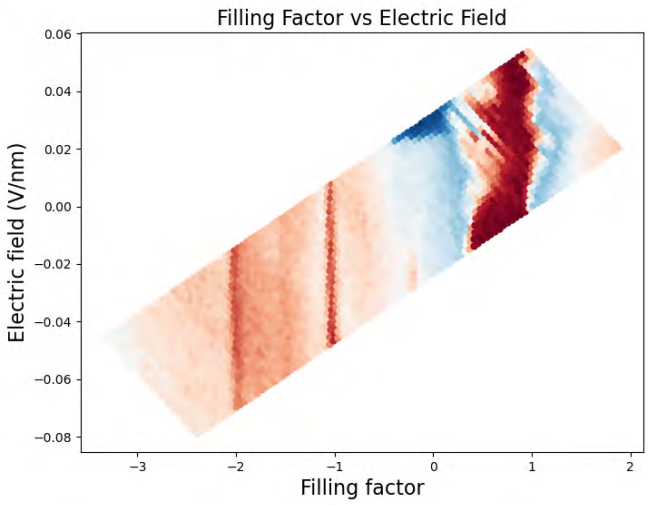

Fig 3. (A) Dual gate measurement with insulating states seen on diagonal lines, (B) filling factor vs electric field plotted from the dual gate measurement with insulating states seen in red.

IV. Conclusion

Twisted double bilayer WSe2 was characterized using the optical response of the 2s exciton in a monolayer WSe2 sensor. Negative gate voltages were used to tune the sample layer filling to the hole side in an attempt to dope the gamma valley. Insulating states were observed at filling factors $\nu = -\frac{1}{3}, -1, -2$ corresponding to a generalized Wigner crystal state, a Mott insulator, and a band insulator. Further study on this system will be needed to confirm that the states observed here are in the gamma valley and to probe for more correlation driven effects.

Acknowledgements

I would like to thank the Mak Shan lab group for guiding my work and for helping me learn about all of the material mentioned in this paper. In particular I would like to thank graduate student Jiacheng Zhu (Raymond), and post doctoral Fellow Patrick Knuppel for being my mentors on this project as none of this would have been achieved without their guidance. I would also like

to thank the Cornell Center for Materials Research for orchestrating the REU program and providing the administrative guidance and funding needed to succeed. This work was supported in part by the Cornell Center for Materials Research with funding from the Research Experience for Undergraduates program DMR-1757420 and DMR-1719875. This work made use of the Cornell Center for Materials Research Shared Facilities which are supported through the NSF MRSEC program (DMR-1719875).

References

[1] Foutty, B. A., Yu, J., Kometter, C. R. *et. al.* Tunable spin and valley excitations of correlated insulators in Γ-valley moiré bands. *Manuscript submitted for publication*. arXiv:2206.10631 [cond-mat.mes-hall] (2022).

https://doi.org/10.48550/arXiv.2206.10631

[2] Tang, Y., Li, L., Li, T. *et al.* Simulation of Hubbard model physics in WSe_2/WS_2 moiré superlattices. *Nature* **579,** 353–358 (2020). https://doi.org/10.1038/s41586-020-2085-3

[3] Xu, Y., Horn, C., Zhu, J. *et al.* Creation of moiré bands in a monolayer semiconductor by spatially periodic dielectric screening. *Nat. Mater*. **20,** 645–649 (2021). https://doi.org/10.1038/s41563-020-00888-y

[4] Kou A., Feldman B. E. *et. al.* Electron-hole asymmetric integer and fractional quantum Hall effect in bilayer graphene. *Science*. **345**, 55-57 (2014). https://doi.org/10.1126/science.1250270

[5] Angeli, M., MacDonald, A. H., Γ valley transition metal dichalcogenide moiré bands. *PNAS*. **118**, 10 (2021). https://doi.org/10.1073/pnas.2021826118

[6] Geim, A.K., Novoselov, K.S., *et. al.* Electric Field Effect in Atomically Thin Carbon Films. *Science* **306**, 666-669 (2004). https://doi.org/10.1126/science.1102896

[7] Wang, L., Meric, I., *et. al.* One-Dimensional Electrical Contact to a Two-Dimensional Material. *Science* **342**, 614-617 (2013). https://doi.org/10.1126/science.1244358

[8] Cao, Y., Fatemi, V., Fang, S. et al. Unconventional superconductivity in magic-angle graphene superlattices. *Nature* **556**, 43–50 (2018). https://doi.org/10.1038/nature26160

[9] Xu, Y., Liu, S., Rhodes, D.A. et al. Correlated insulating states at fractional fillings of moiré superlattices. *Nature* **587**, 214–218 (2020). https://doi.org/10.1038/s41586-020-2868-6